Boundary layer effects on the vortex shedding in a Donaldson-type hydrofoil

A Fontanals[1,2], A Guardo[1,2], A Zobeiri[3], E Egusquiza[1], M Farhat[3] and F Avellan[3]

[1] Centre de Diagnòstic Industrial i Fluidodinàmica, Universitat Politècnica de Catalunya *BARCELONATECH* (UPC-CDIF). Av. Diagonal, 647. 08028. Barcelona, Spain.

[2] Escola Universitaria d'Enginyeria Tècnica Industrial de Barcelona, Consorci Escola Industrial de Barcelona, Universitat Politècnica de Catalunya *BARCELONATECH* (UPC-EUETIB). Fluid Mechanics Department. C\ Compte d'Urgell, 187. 08036. Barcelona, Spain.

[3] Laboratory for Hydraulic Machines. École Polytechnique Fédérale de Lausanne (EPFL-LMH). Av. de Cour 33 Bis. CH-1007 Lausanne, Switzerland.

E-mail: alfredo.guardo-zabaleta@upc.edu

Abstract. Fluid - Structure Interaction (FSI) phenomena is becoming a relevant study field for the design or revamping of hydropower plants. The generalized trend of increasing flow rates and reducing rotor blades/stay vanes thickness in order to improve the efficiency of the machine together with a major push from plant owners/operators for production flexibility (partial load operation is more common nowadays) make the FSI between the vortex shedding phenomenon and the vanes/blades of the machine an area of interest. From a design point of view, the machine structure has to resist all the hydrodynamic forces generated and maintain tension stresses under the fatigue limit to ensure a machine lifetime of several decades. To accomplish that goal, designers have to assure there is no presence of strong coupling phenomena (lock-in) between the vortex shedding frequency and the eigenfrequencies of the structure.

As the vortex street is directly related to the state of the boundary layer along the hydrofoil, in this paper the effect of the boundary layer on the vortex shedding in a Donaldson-type hydrofoil is studied using Computational Fluid Dynamics (CFD). The development of the boundary layer along the Donaldson trailing edge hydrofoil chord is presented under lock-off conditions. The results are validated against previously obtained experimental results. Since the Donaldson trailing edge is non-symmetric, the boundary layer velocity profiles are reported for the suction and pressure side of the hydrofoil. In addition, the effect of the Donaldson trailing edge on laminar-to-turbulent transition on both sides of the hydrofoil is studied.

1. Introduction

Fluid-structure interaction (FSI) is becoming nowadays an important research field on hydraulic machinery design. Operational requirements for fast energy production regulation in hydropower plants lead to an increased availability of the turbines and also wider operation ranges which include in

most of the cases, partial load operation. These factors favor the appearance of higher excitation forces which increase the vibration levels of the machine.

The main goal of this work is to present a numerical study of the flow around a hydrofoil with a Donaldson type trailing edge. Hydrofoils with this type of trailing edges generate a low amplitude vortex shedding what makes them quite interesting to avoid vortex induced vibrations and strong fluid-structure couplings [1] The Donaldson trailing edge is characterized by a progressive smooth change in the slope of the trailing edge in the pressure side of the vane. An existing Donaldson type profile with a chord (**L**) of 100 mm and a maximum thickness (**h**) of 9.9 mm was used for the study. Numerical simulations were carried out using high performance computation (HPC) at the supercomputing facilities of the Consorci de Serveis Universitaris de Catalunya (CSUC) in Barcelona (Spain). The numerical research focuses on the statistical-averaged velocity profiles, thickness and prediction of the laminar-to-turbulent transition in the boundary layer as well as the shedding frequencies.

2. Methodology

2.1. Case study and experimental database

The tested hydrofoil was based on NACA 0009 – 7.8 45/1.93 [2] with a maximum thickness (**h**) equal to 9% of the chord length. The hydrofoil was made of stainless steel with chord and span lengths of 110 mm and 150 mm respectively. NACA 0009 blunt truncated at **L** = 100 mm with trailing edge thickness of 3,22 mm was selected as a reference hydrofoil.

The case study is a Donaldson-type hydrofoil [1]. This hydrofoil is shaped by modifying the blunt trailing edge with a combination of a straight line with an angle of 45º and a 3rd degree polynomial curve (Figure 1). The experimental database used to validate the numerical results presented in this work was obtained in the hydraulic tunnel of the Laboratory for Hydraulic Machines located in the École Polytechnique Fédérale de Lausanne (EPFL-LMH), Switzerland. For more insight on the technical specifications of the hydraulic tunnel please refer to [3]. Detailed information about the experimental database can be found in [4].
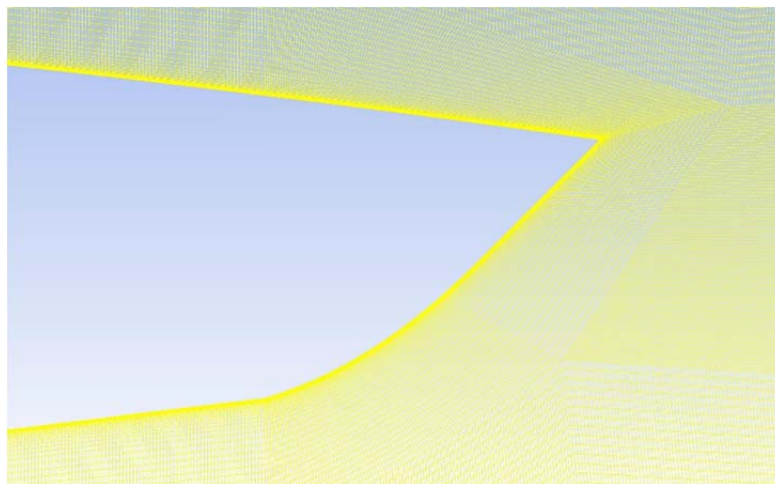

Figure 1. Trailing edge geometry and mesh detail for the Donaldson-type hydrofoil.

2.2. Numerical procedure

The unsteady numerical simulations were performed using the commercial software ANSYS FLUENT 13®, based on the finite volume method, which solves simultaneously the momentum and

the mass conservation equations for a fluid. The set of equations is closed-formed and is solved using a turbulence model. The equations were discretized using the backward Euler implicit scheme, second order in time and second order in space.

The rectangular computational domain of the 3D hydrofoil was discretized with a structured mesh, as seen in Figure 1. Time step for the numerical simulations was set to be $\Delta t = 1 \times 10^{-5}$ s after performing a time-step sensitivity test. Boundary conditions were imposed as follows: no-slip condition at the hydrofoil wall; uniform velocity $c_{ref} = 20$ m/s in the *x* direction fixed at the inlet with a turbulence intensity of 1 %; a constant average static pressure imposed at the outlet; symmetry boundary conditions at all other surfaces of the computational domain.

HPC was used to solve the numerical models. Simulations were carried out in a SGI Altix UV 1000 supercomputer property of CSUC, with an average computation time (per 10000 iterations) of 60 - 110 CPU hours depending on the turbulence model used. Time-averaged velocity profiles, obtained after lift coefficient, drag coefficient and flow rate at the outlet showed a pseudo-steady behavior, were recorded for the boundary layer. Lift coefficient time signals were used to determine shedding frequencies in each case studied by means of a Fast Fourier Transform algorithm (FFT) [5]. Obtained numerical results were compared against experimental results for velocity profiles and vortex-induced vibration in the hydrofoil.

3. Results and discussion

Figure 2 presents the non-dimensional time-averaged boundary layer x component of velocity, ($c_{x,mean}/c_{ref}$) profiles in the boundary layer at *x/L*=0.2, 0.4, 0.5, 0.6, 0.7, 0.8 and 0.9 of the hydrofoil chord length (where **L** is the chord length, **h** is the maximum thickness of the studied hydrofoil, and c_{ref} the uniform stream wise velocity at the inlet) obtained using four different turbulence modeling approaches.
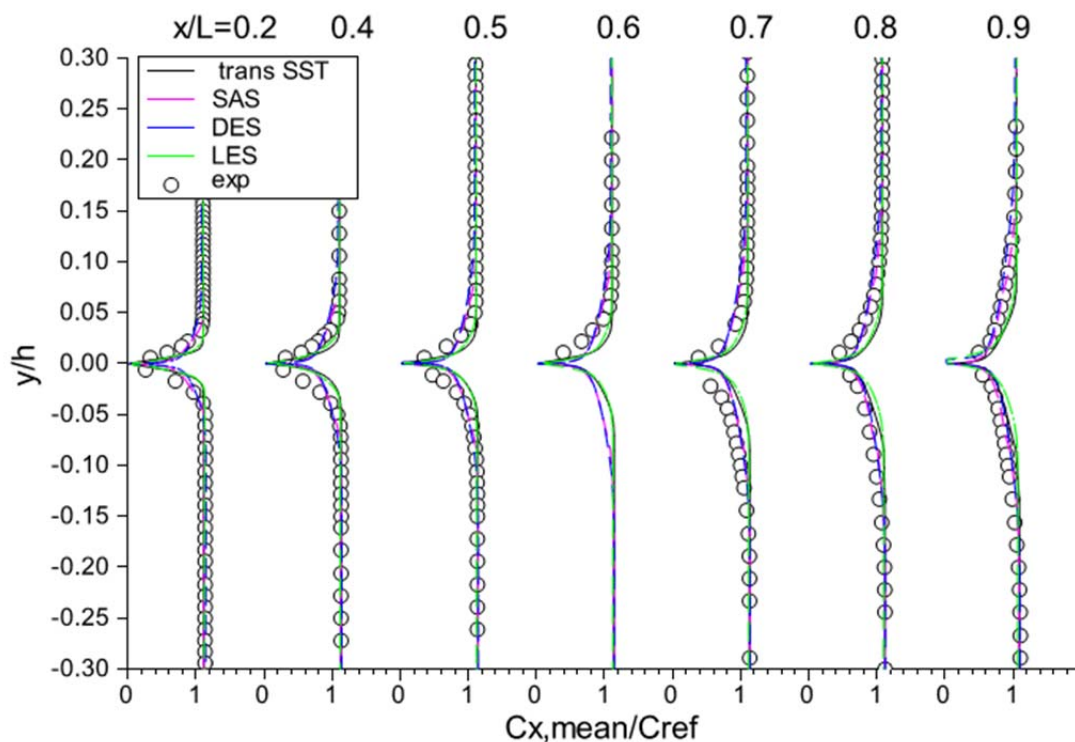

Figure 2. Time-averaged boundary layer *x* component velocity profiles, at different positions along hydrofoil.

The comparison between the boundary layer velocity profiles on the suction (upper) and pressure (lower) sides of Donaldson trailing edge (Figure 2) reveals a thicker boundary layer on the pressure side of the hydrofoil. In addition, laminar-to-turbulent transition occurs earlier on the hydrofoil pressure side, where a fully turbulent boundary layer velocity profile is achieved at 50 to 70% of the chord length, while for the suction side the transition is observed at 60% to 80% of the chord length.

The numerical results obtained for the boundary layer velocity profiles (Figure 2) show that large eddy simulation (LES) and transitional SST k-ω (Trans-SST) predict the laminar-to-turbulent boundary layer transition closer to the hydrofoil's leading edge, while detached eddy simulation (DES) or a scale-adaptive model (SAS) predict this flow transition past the experimental transition zone on a point closer to the trailing edge. DES and SAS models predict the laminar-to-turbulent transition at around 40% of the chord length, which leads to an overestimation of the boundary layer thickness at the detachment point (Figure 3).

The laminar-to-turbulent transition prediction and the boundary layer thickness at the detachment point of the trailing edge have a direct effect on the vortex shedding frequency captured by the numerical model. Lift coefficient time signals were used to determine shedding frequencies in each case studied by means of a Fast Fourier Transform algorithm (FFT) [5]. The results obtained are shown in Table 1. It can be observed that a thicker boundary layer prediction results in a lower numerical shedding frequency (Table 1) and a greater numerical error. Among the turbulence models tested, LES modeling shows the lower numerical error in the shedding frequency prediction.
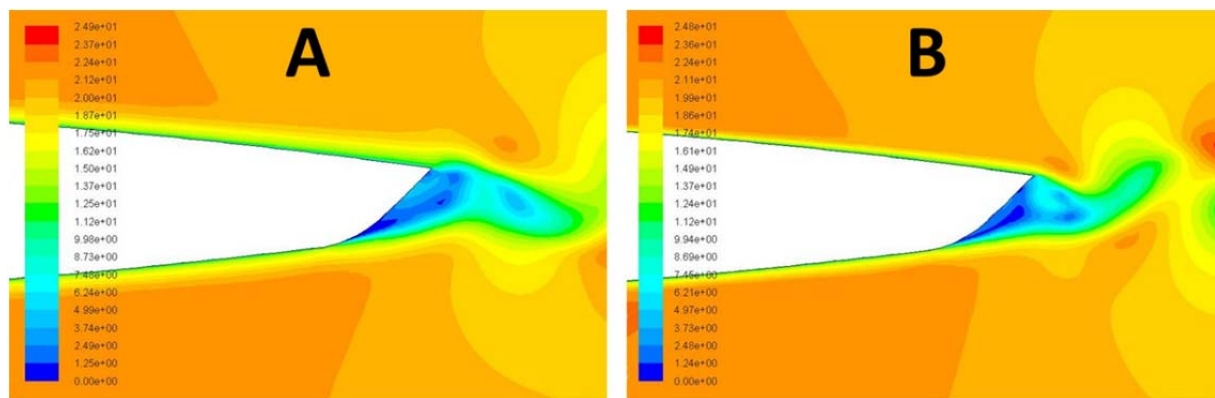

Figure 3. Velocity contours in the trailing edge of a Donaldson-type hydrofoil using (A) SAS and (B) Trans-SST turbulence models.

Table 1. Vortex shedding frequencies obtained for C_{ref} = 20 m/s

Turbulence model	Experimental (Hz)	Numerical (Hz)	Error (%)
Trans-SST		1431	22,2
SAS	1840	1231	33,1
DES (SST submodel)		1224	33,4
LES (WALE)		1491	18,9

For all cases studied, a power spectra density study at different locations of the boundary layer was performed. In the spectrum of Figure 4, a regular decay of slope close to −5/3 is observed over more than one decade in the frequency. This is indicative of an inertial subrange, a necessary condition for the flow to behave like locally isotropic turbulence. However, it can also be observed that Trans-SST turbulence model is able to capture differences in the boundary layer development for the suction and pressure sides reported by experiments, while SAS model shows a similar behavior for both sides of the hydrofoil.
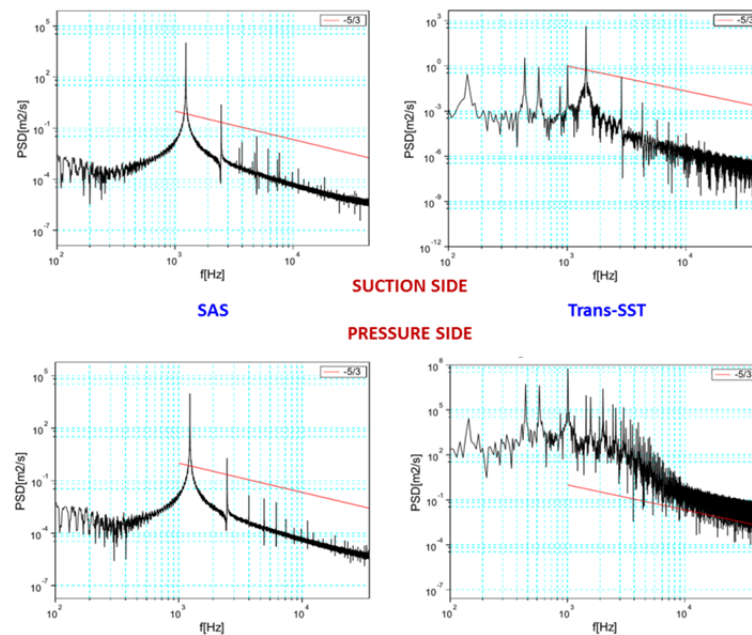

Figure 4. Power spectrum density analysis of the streamwise velocity fluctuation at the boundary layer outer sublayer at 50% of the hydrofoil chord.
Up: suction side; down: pressure side; left: SAS model; right: Trans-SST model.

4. Conclusions

Computational fluid dynamics proves to be a suitable tool to model the boundary layer flow and vortex shedding effects around hydrofoils. A Donaldson-type hydrofoil was studied by means of CFD, and the time-averaged boundary layer velocity profiles and vortex shedding frequencies were obtained using four different turbulence models. Numerical results obtained were compared against previously-obtained experimental results for validation.

Results obtained show that the laminar-to-turbulent transition occurs earlier on the hydrofoil pressure side. From the four different turbulence models used for modeling, transitional SST k-ω and large eddy simulation are more accurate for estimating the time-averaged velocities in the boundary layer. Detached eddy simulation and the scale-adaptive model predict the laminar-to-turbulent transition at around 40% of the chord length, which leads to an overestimation of the boundary layer thickness at the detachment point. The boundary layer thickness predicted for the detachment point at the trailing edge of the hydrofoil has a direct effect on the shedding frequency obtained.

References
[1]   Donaldson R M 1956. Hydraulic turbine runner vibration. *Journal of Engineering for Power* 78, 1141 – 1147
[2]   Abbott I H, Von Doenhoff A E and Stivers L S Jr. 1945. Summary of Airfoil Data. *NACA Rep. No. 824*
[3]   Avellan F, Henry P and Rhyming I 1987. A new high speed cavitation tunnel for cavitation studies in hydaulic machinery. *American Society of Mechanical Engineers, Fluids Engineering Division FED* 57, 49 – 60
[4]   Zobeiri A 2012. Effect of hydrofoil trailing edge geometry on the wake dynamics. *Ph.D. Thesis.* (Switzerland: École Polytechnique Fédérale de Lausanne)
[5]   Cooley J W and Tukey J W 1965. An algorithm for the machine calculation of complex Fourier series. *Mathematics of Computation* 19, 297 – 301